Vol. 18, No. 1, 2026, pp. 149–169 ISSN (Print): 2008-7306 ISSN (Online): 2423-5865

Journal of Economic Geology

https://econg.um.ac.ir

RESEARCH ARTICLE 10.22067/econg.2026.1164 OPEN ACCESS

Hydrothermal Fluid Evolution based on Stable Isotopes (S, O, D) and Fluid Inclusion studies in the Masjeddaghi Porphyry (Cu-Au) System, NW Iran

Shohreh Hassanpour [1] *, **Seyed Javad Moghaddasi** [2]

[1] Associate Professor, Department of Geology, Payame Noor University, Tehran, Iran
2 Associate Professor, Department of Geology, Payame Noor University, Tehran, Iran

ARTICLE INFO

Article History

Received: 01 December 2025
Revised: 22 April 2026
Accepted: 27 April 2026

Keywords

Sulfur
Oxygen and hydrogen isotopes
Fluid inclusion micro thermometry
Masjeddaghi
NW Iran

ABSTRACT

The Masjeddaghi deposit, located in northwest Iran, comprises a porphyry Cu–Au system, spatially associated with epithermal silica replacement and vein-type mineralization. The intrusion-volcanic complex in the area formed during the early Eocene and consists of quartz–diorite to diorite. Geochemically the diorites have island arc affinities and are enriched in LILE (large-ion lithophile) elements like Y, Th, Rb, Ba, and Cs, due to subduction-related mantle contamination. Primary fluid inclusion in porphyry-hosted veinlets homogenize into both liquid and vapor at temperatures ranging from 189˚C to 585˚C and yield salinities between 0.3 to 59 wt.% NaCl equivalent indicating fluid boiling and phase separation. The isotopic composition of the fluid (δD = –60 to –30 ‰, $\delta^{18}O$= 4.3 to 11.9 ‰) suggests a dominantly magmatic origin with limited meteoric water involvement. These results indicate that high-temperature, saline magmatic fluids played a primary role in copper–gold mineralization at Masjeddaghi.

***Corresponding author**

Shohreh Hassanpour
✉ hassanpour@pnu.ac.ir

How to cite this article

Hassanpour, Sh. and Moghaddasi, S.J., 2026. Hydrothermal Fluid Evolution based on Stable Isotopes (S, O, D) and Fluid Inclusion studies in the Masjeddaghi Porphyry (Cu-Au) System, NW Iran. Journal of Economic Geology, 18(1): 149–169. (in English with Persian abstract) https://doi.org/10.22067/econg.2026.1164

Introduction

Porphyry copper systems represent one of the most economically significant sources of copper and gold worldwide and are typically characterized by large halos of zoned alteration assemblages.

The Masjeddaghi porphyry system is located in NW Iran and was selected as a case study due to its extensive, well-exposed alteration halos covering more than 1 km² and the preservation of potassic and propylitic alteration zones to depths of approximately 1000 m (Fig. 1). The geology, alteration and mineralization characteristics of the deposit have been studied extensively by Akbarpour (2005); NICICO (2008); Hassanpour and Rajabpour (2019); Hassanpour et al. (2022); Hassanpour and Alirezaei (2017); Akbarpour (2005) and Atalou et al. (2017). Therefore, the geochemistry, geology and geochronology of the region are well-understood from surface work and drilling (Hassanpour and Alirezaei, 2017; Ebrahimi et al., 2021). These studies established a subduction-related island-arc affinity for the causative intrusions and confirmed the presence of multi-stage hydrothermal activity. However, despite these contributions, the source, evolution, and temporal variation of hydrothermal fluids—particularly as constrained by integrated stable isotope and fluid inclusion data—remain incompletely understood. The mineral assemblages, their zoning, and paragenesis of the hydrothermal minerals, fluid inclusion and hydrothermal evolution history of the porphyry have been studied completely by (e.g Hassanpour and Alirezaei, 2017; Ebrahimi et al., 2021; NICICO, 2008). Combining of these studies with laboratory results have led to improved application for exploration and detecting concealed porphyry ore deposits. All the above exploration and detailed studies on the origin of the deposit are reviewed by Hassanpour and Alirezaei (2017); Hassanpour and Ebrahimi (2023); Ebrahimi et al. (2021) and NICICO (2008) and are references herein.

The genesis of the porphyry system and nature of the hydrothermal fluids (magmatic and meteoric waters) are related to potassic, sericite and advanced argillic alteration assemblages. Based on hydrogen and oxygen isotope studies of porphyry ore deposits in North America, it was proposed that the solutions responsible for development of phyllic alteration were dominated by meteoric waters (Taylor, 1974; Sheppard et al., 1969; Sheppard et al., 1971; Calagari, 2004; Hassanpour, 2010; Hassanpour et al., 2015; Hassanpour and Ebrahimi, 2023). However, Kusakabe et al. (1990) believed that the fluid responsible for forming phyllic alteration at the Rió Blanco and El Teniente deposits in Chile, were magmatic in origin. Hedenquist and Richards (1998) believed that in the Lepanto and Far Southeast deposits (Philiipines), K silicates and advanced argillic assemblages shared a magmatic origin and formed at the same time, at about 1.4 Ma. Advanced argillic alteration was thought to originate from a magmatic vapor which condensed into meteoric waters. Phyllic alteration formed about 100,000 years later from magmatic fluids. The evolution from early K-silicate to late sericitic alteration stages correlated with a transition from magmatic fluids under lithostatic pressure with dominantly meteoric water at hydrostatic pressures Hedenquist and Richards (1998). This process propably occurred with changes from discontinuous ductile-brittle fractures to continuous brittle fractures, facilitated by the last intrusion (Gustafson and Hunt, 1975). Sheppard and Gustafson (1976) approved these conclusions with their observations and interpretations of hydrogen and oxygen isotopic compositions.

Petrological study of the Masjeddaghi intrusive shows its meta-aluminous with high K-shoshonitic to calc-alkaline features (Hassanpour and Alirezaei, 2017). Composition of the intrusive rocks are classified as quartz–diorite to diorite, and plot in the sland arc field on tectonic discrimination diagrams. The intrusions are enriched in large ion lithophile elements including Y, Ba, Th, Cs and, Rb (LILE) due to contamination of the mantle wedge by crustal material as a resultof the subduction-related setting (Hassanpour and Alirezaei, 2017; Davidson, 1996; De Hoog et al., 2001). The depletion of high field-strength element (HFSE) (e.g. Ti and Nb) is significant and is thought to related to the relatively immobile nature of these elements during partial melting processes subduction zone settings (Hassanpour and Alirezaei, 2017; Brenan et al., 1994; Foley et al., 2000).

This study aims to address by integrating fluid inclusion microthermometry with oxygen, hydrogen, and sulfur isotope analyses from alteration minerals and sulfides across different alteration zones in the area. The primary objectives are to characterize the temperature–salinity evolution of hydrothermal

fluids, constrain the relative contributions of magmatic and meteoric waters, and evaluate the role of fluid processes such as boiling and mixing during copper–gold mineralization. The results provide new insights into the genetic model of the Masjeddaghi porphyry system and contribute to a broader understanding of fluid evolution in porphyry Cu–Au deposits worldwide

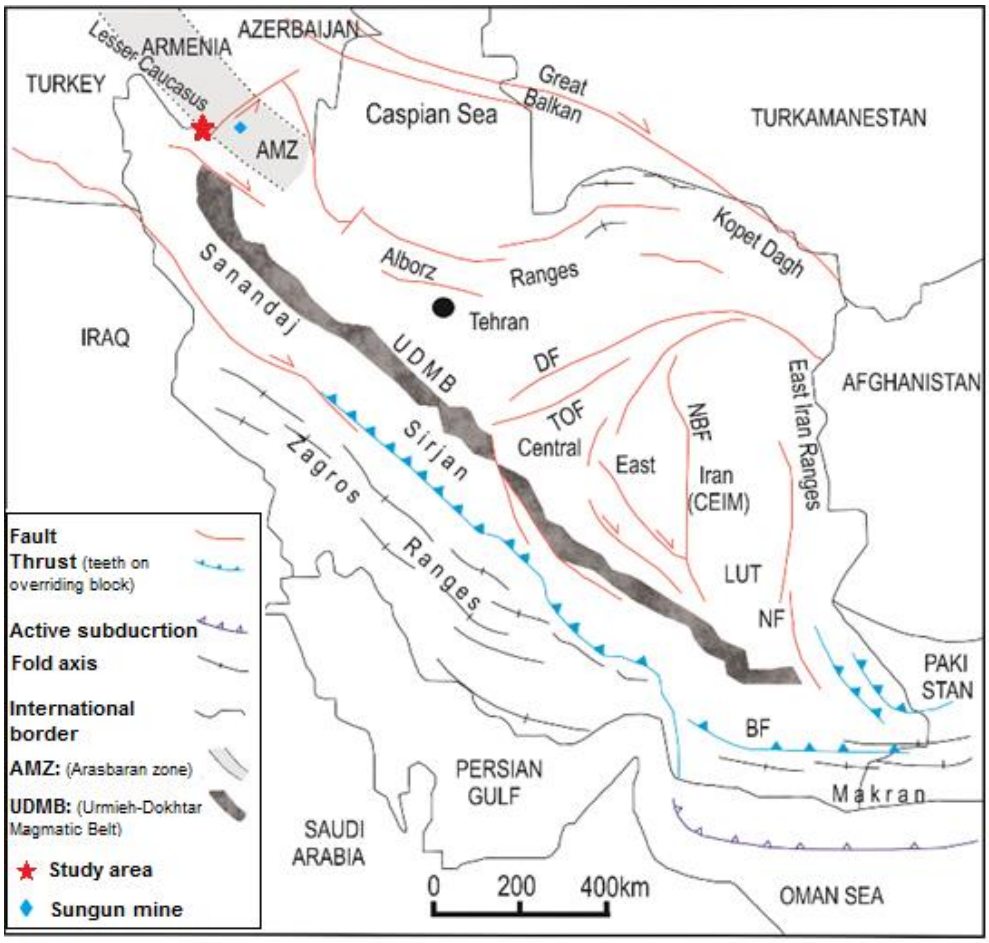

Fig. 1. Structural geology map of Iran, showing the tectonic setting of the Masjeddaghi porphyry Cu–Au (modified after, Stocklin and Setodehnia, 1972)

Geology and Structure

The geological setting of Masjeddaghi is shown in Fig. 2, based on mapping and studies from multiple sources (GSI, 1999; Hassanpour et al., 2022). The southeastern and eastern exposures are dominated by Paleocene andesitic lava flows and associated volcaniclastic rocks that overlie a basement of Permian-Triassic age (Fig. 3A). The central part of Masjeddaghi is composed of a mineralized dioritic stock, dated between 55 and 60 Ma, which constitutes the primary host rock to mineralization (Hassanpour et al., 2022; Fig. 3B). This stock is intruded by east–west–trending Middle Eocene diorite porphyry that, exhibits granular to porphyritic textures (Fig. 3C). The magmatic activity responsible for these rocks, along with the coeval Cu-Mo-Au mineralization and alteration, occurred at approximately 54 Ma (Hassanpour et al., 2022; Hassanpour and Alirezaei, 2017; Fig. 3D)

The diorite porphyry complex contains multiple intrusive units and extends across the study area from north to south. The present study includes samples collected at the surface and from depth in this porphyry system.

West–east trending andesitic dikes that crosscut the diorite mineralized porphyry complex represent a later magmatic event in (Fig. 3C).

Hydrothermal breccia and brecciated diorite porphyry crop out at the surface. The breccia consists of fragments of diorite porphyry and andesitic cemented by quartz. Silica ledges are present in diorite porphyry and form part of the epithermal system located in the northeastern part of the area (Fig. 3C).

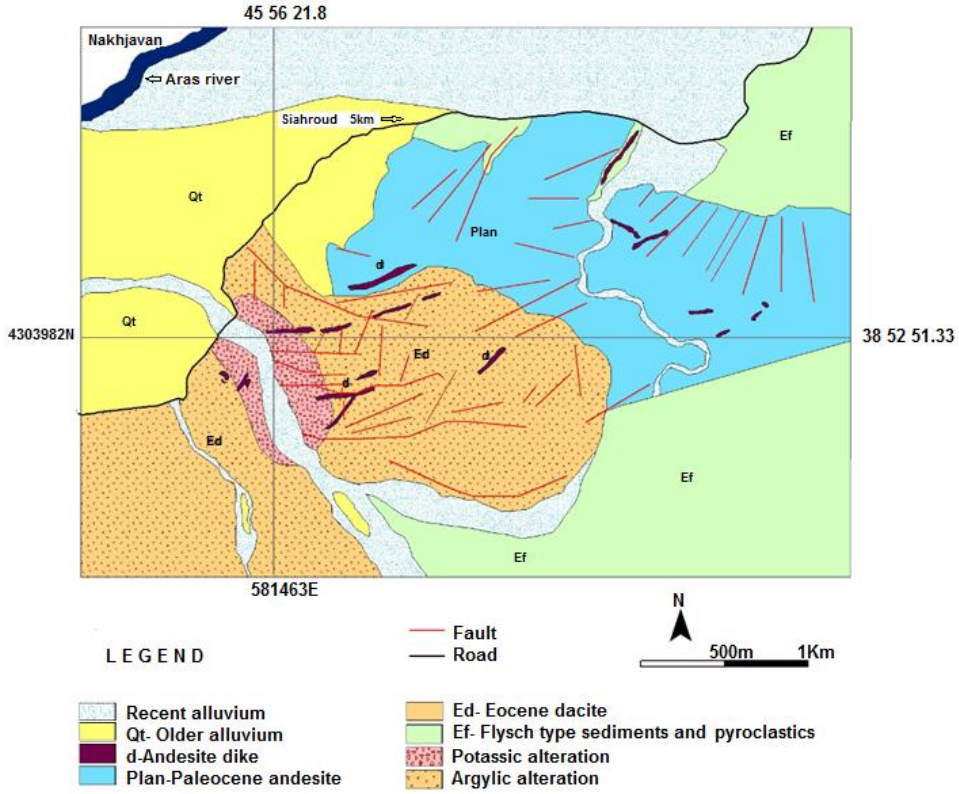

Fig. 2. The geological map of the Masjeddaghi (modified after GSI, 1999) by Hassanpour and Alirezaei (2017)

Alteration and Mineralogy

Potassic and propylitic alteration are the dominant alteration assemblages developed within the Masjeddaghi ore deposit (Fig. 4A). (Fig. 4A). Minor, patchy occurrences of phyllic alteration are locally observed in drill cores within the surrounding andesitic unit. XRD and petrographic analyses indicate that potassic and propylitic alteration are predominantly developed within the diorite porphyry intrusion. The propylitic alteration zone is developed into the andesitic country rocks (Fig. 4B). The widespread exposure of potassic alteration outcrops indicates a deep erosional level, suggesting that the upper parts of the porphyry system have been extensively removed. The diorite porphyry stock is the main intrusive stock in the Masjeddaghi deposit, and was emplaced in the early Eocene (~54 Ma; Hassanpour and Alirezaei, 2017; Fig. 4A). A range of quartz veinlets and potassic and propylitic alterationoccurs within the porphyry stock. The dominant copper mineralization is mainly present in the potassic alteration zone.

Based on microscopic studies, the quartz–diorite to diorite porphyry rocks have porphyritic textures with course- to medium-grained plagioclase, quartz, K-feldspar, and amphiboles in association with fine-grained, secondary euhehdral biotite crystals (Fig. 4C). Potassic alteration within central drill cores is dominantly composed of secondary hydrothermal biotite, euhedral fine–grained K–feldspar and silica

(Fig. 5A, H, I, J) and is associated with some patches of phyllic alteration (Fig. 5B). Opaque minerals including pyrite, magnetite, chalcopyrite, and molybdenite occur within this area (Fig. 5C).

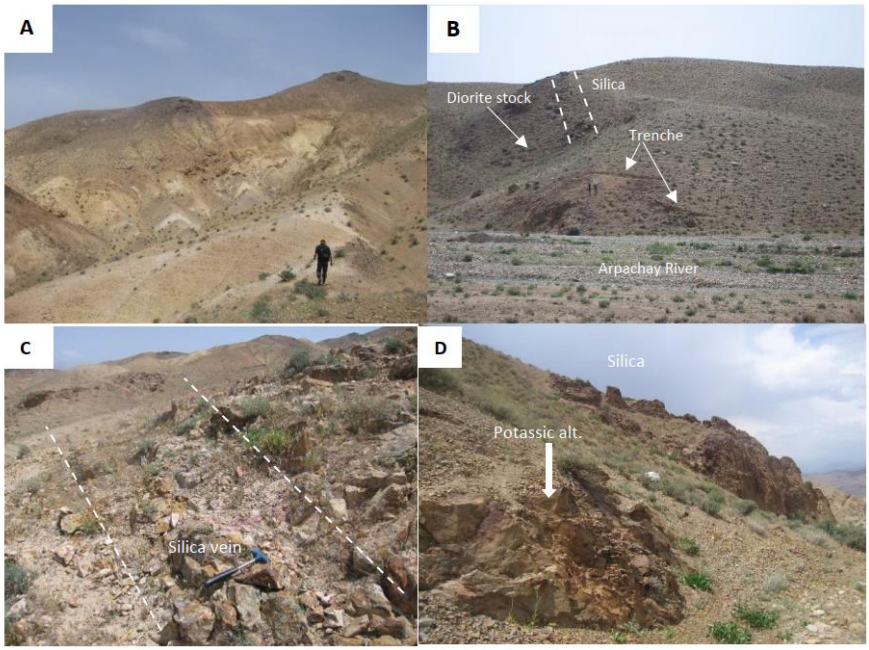

Fig. 3. Some viewpoints of the Masjeddaghi district. A: Andesite volcanic rocks (lavas, pyroclastic, and epiclastic rocks) lied on Permian- Triassic rocks, B: Diorite porphyry stock with silicic veins which form part of an epithermal gold-bearing system. Trenches are located near the base of the hill, C: Silica ledges in the upper part of the Masjeddaghi porphyry system in the north and northeastern parts, and D: Pinkish colored potassic alteration zone in association with stockworks of K-feldspar-quartz veins and veinlets

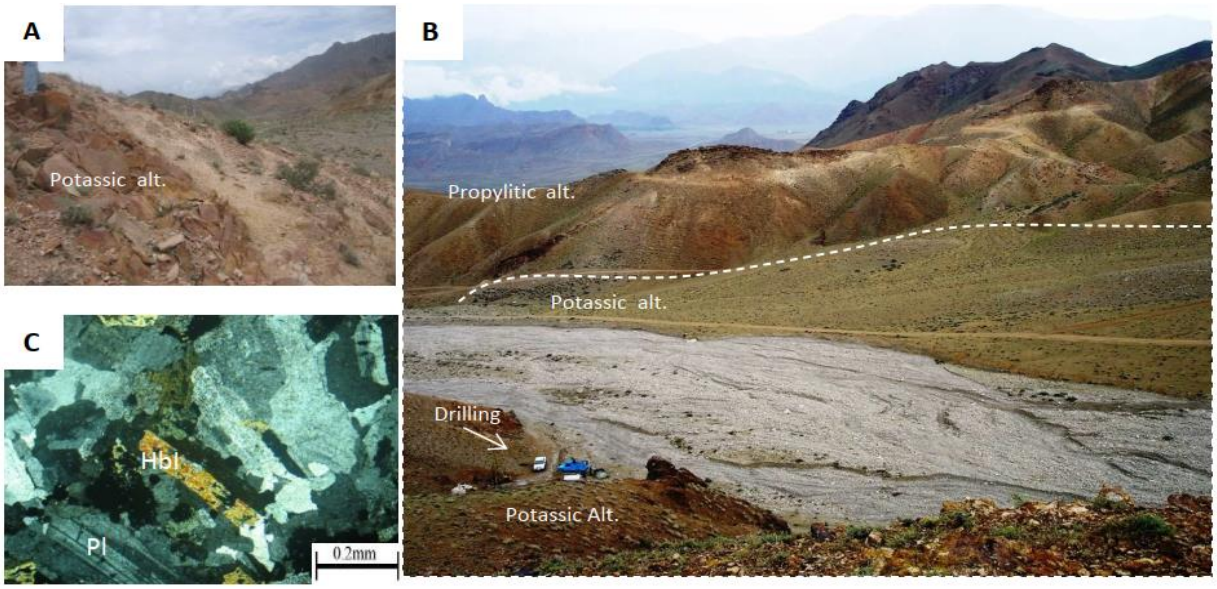

Fig. 4. A: Potassic alteration zone outcrop (pink) in the Masjeddaghi porphyry system, B: The main alteration zones comprise potassic and propylitic alteration in the study area, and C: Microscopic texture of diorite porphyry in the area, composed of plagioclase, quartz and ferromagnesian minerals like, amphibole, biotite and rutile. Abbrevations after Whitney and Evans (2010) (Pl: plagioclase, Hbl: hornblende, alt: alteration).

The phyllic alteration zone is weakly developed and occurs in patchy form, consisting of sericite replacing primary feldspar. Plagioclase and ferromagnesian minerals are partially or completely replaced by quartz and sericite. Veinlets composed of pyrite or quartz–pyrite-chalcopyrite are associated with molybdenite veinlets, disseminations, and open spaces fillings (Fig. 5C, D, E, F, and G), comprising up to 20-25 vol. % of the rocks. The propylitic alteration zone crops out along the margins of the ore deposit and is dominated by chlorite, calcite, pyrite and magnetite. Chloritization of ferromagnesian minerals and formation of calcitic veinlets within the stock are the most important processes in this zone.

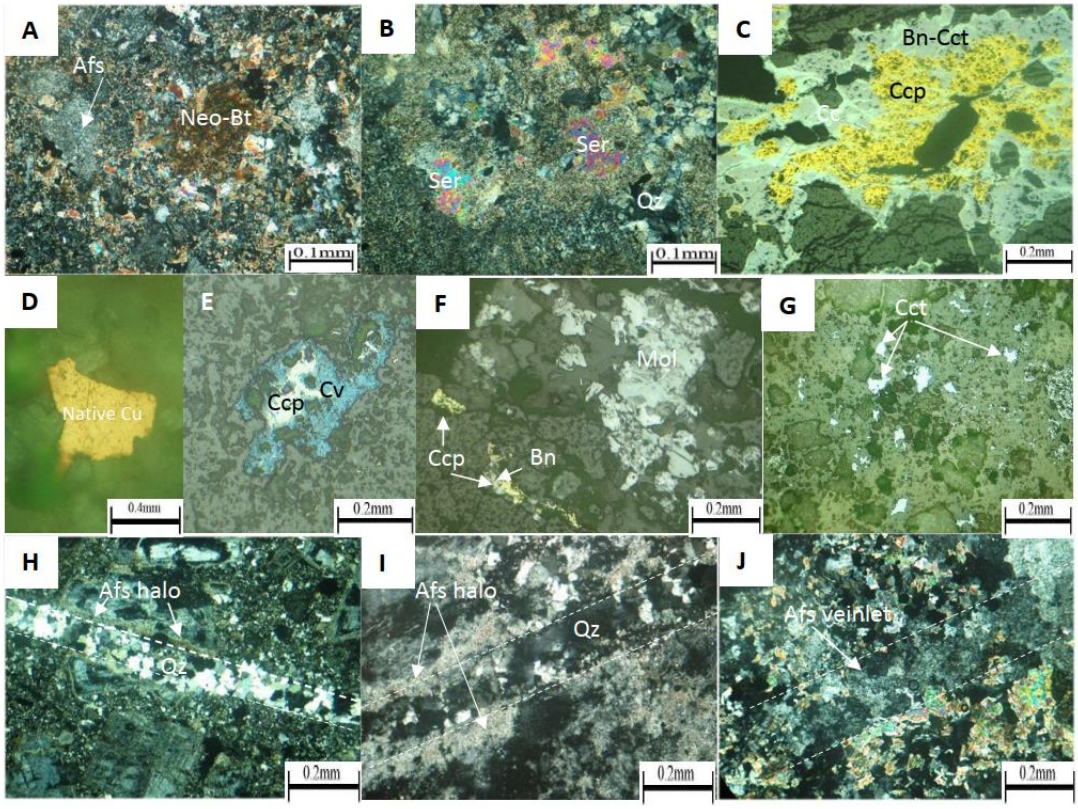

Fig. 5. Photomicrographs A: Potassic alteration with neo-formed biotite, and alkali feldspar as veinlets or dissemination in the Masjeddaghi porphyry system, B: Phyllic alteration as small patches that overprinted potassic alteration zones with sericite, quartz and pyrite, C: Mineralization in the Masjeddaghi porphyry system comprised of bornite, chalcopyrite, and chalcocite, D: Native copper as a rare event in the Masjeddaghi porphyry system, E: Chalcopyrite which is partly altered to covellite, F: Bornite, chalcopyrite and molybdenite, G: Primary chalcocite in the Masjeddaghi porphyry system, H: A type veinlet in the study area, a quartz veinlet that is surrounded by K-feldspar haloes, I: A quartz veinlet with K-feldspar haloes, and J: K-feldspar halo around the veinlet with sericite in the matrix overprinting potassic alteration. Abbrevations after Whitney and Evans (2010) (Afs: alkali feldspar, Neo-Bt: Neo-biotite, Ser: Sericite, Qz: Quartz, Bn: Bornite, Ccp: Chalcopyrite, Cct: Chalcocite; Cv: Covellite, Mol: Molybdenite, Cu: Copper).

Quartz veins

According to crosscutting relationships of veinlets, most of the types of veinlets which are identified in typical porphyry systems are present associated with mostly potassic, silicic and phyllic alteration zones, respectively (Fig. 5H, I and J): (i) A type quartz veinlets associated with potassic alteration, (ii) B type quartz veinlets composed of pyrite + quartz + chalcopyrite ± molybdenite within phyllic alteration zones (iii) C type quartz veinlets dominated by pyrite, being identified in the potassic and phyllic alteration zones, (iv) D type quartz veinlets

containing anhydrite and minor amounts of pyrite, observed mainly near the dioritic porphyry stock. These veinlets vary from around 1 millimeter to several millimeters in thickness. Sulfide minerals and quartz within these veinlets commonly contain abundant fluid inclusions and were therefore selected for microthermometry analysis. Fig. 5 represents mineralization stages and the paragenetic sequence of the mineralization in the Masjeddaghi porphyry system.

Samples and Analytical Methods

In order to understand the physicochemical nature of ore formation, fluid inclusion studies were conducted on double–polished thin sections of the samples which contain sulfide- rich quartz veinlets in potassic alteration in outcrops and/or drill holes in the Masjeddaghi porphyry system. Fluid inclusion studies were carried out in Mineralogical Laboratory in Advanced Research Center for Ore Materials (ARCOM) in Karaj city, Iran. We have also used a few of the fluid inclusion results from the phyllic alteration zone carried out by (Ebrahimi et al., 2021; ten double polished sections). In this research, fluid inclusion microscopic study was conducted on five samples from potassic alteration and five samples from phyllic alteration zones using an Olympus microscope. Microthermometric analyses were carried using a Linkam THMS600 heating and freezing stage system. The instrument accuracy is ± 0.1 °C, and the heating range is from –180 to + 600 °C. The equipment consists of two TP94 LNP cooling and heating controllers, nitrogen (for freezing) and water tanks (to cool from high temperatures). Measurements on two phase halite-bearing fluid inclusions included homogenization temperatures of liquid and vapor phases or Th (LV) and temperatures of halite dissolution Th (NaCl). that the concentrations of NaCl and KCl were estimated using eutectic temperatures (T_e) (IMPRC, 2026). The density of fluid inclusions were calculated based on Zhang and Frantz (1987).

For the study of hydrogen, oxygen, and sulfur isotope compositions, twelve representative samples of pyrite, chalcopyrite, and biotite were carefully separated from potassic alteration and five samples of sericite were obtained from phyllic alteration zones. To determine the origin of fluids in the Masjeddaghi deposit, twenty-two samples were selected based on detailed microscopic examination and carefully hand-picked using a binocular microscope in Tehran, Iran. The samples were then ground to 20 mesh and washed with distilled water in preparation for isotope analysis. At Queen's University, Canada, the samples were analyzed for sulfur, oxygen, and hydrogen isotopes. Hydrogen and oxygen isotopic measurements are performed on ten biotite and sericite samples from the potassic and phyllic alteration zones, respectively, using a Finnigan Delta Plus XL mass spectrometer with a dual-inlet Gas Bench II. The results for oxygen and hydrogen are expressed as $\delta^{18}O$ and δD values in per mil (‰) relative to the V-SMOW standard. All measurements had an analytical precision of better than ±0.1‰ (1σ).

Mass spectrometric analysis of twelve sulfide samples (eight pyrite and four chalcopyrite) was conducted using a Delta C Finnigan MAT continuous flow isotope ratio mass spectrometer. The sulfur isotope composition is reported in standard $\delta^{34}S$ notation, representing per mil (‰) deviations from the Vienna-Canyon Diablo Troilite (V-CDT) standard. Analyses were performed at the Queen's University Lab.

Results

Fluid inclusions

Fluid inclusion studies

The thermodynamic conditions of the deposit were constrained using fluid inclusion studies on quartz from veinlets in the phyllic and potassic alteration zones. Microthermometric analyses were carried out on primary fluid inclusions. Their shapes were elongated, irregular, and rounded which are features of primary inclusions according to Shepherd et al. (1985) and Roedder (1984). Three types of fluid inclusions were identified in Masjeddaghi: (1) liquid rich (LV; Fig. 6A, C, and E), (2) halite bearing liquid rich (LVHa) (Fig. 6B) (3), and multiphase (LVS) (Fig. 6D and F) inclusions. However, some single phase liquid and vapor-rich CO_2 bearing fluid inclusions are also observed in potassic and phyllic alteration zones.

In this research, fluid inclusion microthermometry was conducted on multiphase LVS, primary LV, and LVHa fluids (Fig. 6), and also incorporates data modified after Ebrahimi et al. (2021). Two phase LV inclusions (L>V; with sizes between 11 to 15 μm) were homogenized to liquid in all quartz vein types. LVHa inclsions range from 11 to 13 μm in size and

contain daughter minerals such as halite, sylvite and anhydrite and opaque minerals like (chalcopyrite, hematite) (Ebrahimi et al., 2021).

The presence of chalcopyrite and other opaque daughter minerals indicates that the inclusions contain samples of metal-bearing hydrothermal fluids.

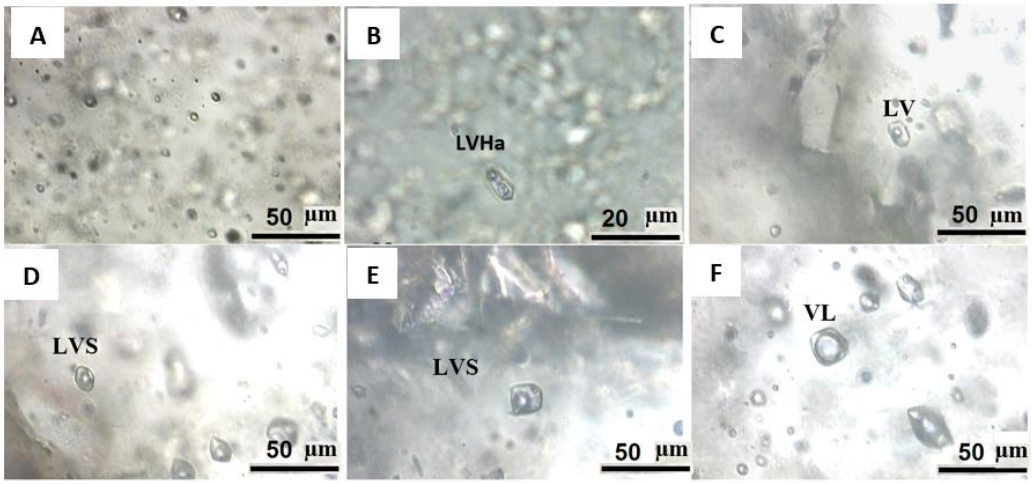

Fig. 6. Type of fluid inclusions and assemblages at Masjeddaghi porphyry system. A: Some secondary liquid rich halite bearing liquid-rich? (LVHa) inclusions, B: primary liquid rich and halite bearing inclusions (LVHa), C: Primary liquid rich inclusions (LV), D and E: primary multiphase (LVS) inclusions of clearly visible halite daughter minerals, and F: the existence of primary vapor-rich and liquid-rich fluid inclusion assemblages indicated boiling conditions

Fluid inclusions micro-thermometry

Micro-thermometric data collected from different stages of mineralization are presented in Table 1; Figs. 7 and 8. All inclusions (23 inclusions) studied in mineralized rocks are in quartz veinlets. The homogenization temperatures of primary LV fluid inclusions range from 189 to 222°C with an average of about 200°C and one LV had a homogenization temperature of >550°. Calculated salinities for these LV inclusions range from approximately 2.5 to 3.78 wt.% NaCl equivalent. Multiphase inclusions (LVHa and LVS) homogenized by halite dissolution ($Th_{(NaCl)}$]; Table 1; Fig. 6B) at 192°C to 585 °C with an average of 388°C. The salinities in this group are about >0.3 to 59 wt.% NaCl equivalent. The salinities of LVS inclusions were calculated by using of dissolution temperature of halite daughterminerals. The alinity of multi-phase LVS fluid inclusions ranges between 20 and 59 wt.% NaCl equivalent (Fig. 6D; Fig. 7A and B).

Oxygen and hydrogen isotopes

Oxygen and hydrogen isotopes provide key constraints on the sources and evolution of hydrothermal fluids (e.g. Dilles, 1992). Ten samples from surface and drill holes number 1 and 2 were selected for sericite and biotite analysis and the oxygen and hydrogen isotope data are presented in Table 1.

The $\delta^{18}O$ values were calculated using mean values of the homogenization temperatures of fluid inclusions in this study. The biotite samples yield $\delta^{18}O$ values ranging from 3.0 to 7.2 ‰ (average 5.1‰) and δD values from -91 and -68‰, (average –79 ‰). Calculated $\delta^{18}O$ values for fluids in equilibrium with biotite range from 1.8 to 6.2‰ (Table 2; Zheng, 1993; Bottinga, and Javoy, 1975). The sericite samples showed $\delta^{18}O$ values ranging from 19.6 to 9.4‰ (average 8.8‰) and their δD values vary between –83 and –54‰ with average of about –70.8‰. Calculated isotopic composition for fluids in equilibrium with sericite have δD_{H2O} values –60 to –31‰ (Suzuoki and Epstein, 1976) and $\delta^{18}O_{H2O}$ values vary from 8.7 to 18.2‰ (Zheng, 1993; Table 2).

Table 1. Oxygen and hydrogen analysis data from Masjeddaghi porphyry system

Sample	Mineral	T	Yield	d^{18}O(VSMOW)	^{18}O	Wt.%H2O	dD(VSMOW)	^{2}D
Msj2	Sericite	270	6.8	12.4	11	1	-60	-37
Msdgx	Biotite	420	12.8	3.9	1.8	2.5	-91	-53
Msdggi5	Sericite	270	15.1	19.6	18.2	4	-54	-31
Msdg15	Biotite	420	13.1	6	3.9	7.1	-68	-30
Msdg14	Sericite	270	14.4	10.8	9.4	3.1	-83	-60
Mad-02-309	Sericite	300	15.3	12.6	11.9	4.4	-63	-40
Mad-02-392	Biotite	500	13.1	6.7	4.3	3.7	-75	-41
Mad-02-55	Biotite	450	13.6	8.6	6.2	5	-83	-49
Mas-01-118	Biotite	500	13.2	7.2	4.8	3.6	-74	-39
Mas-01-118	Sericite	380	14.8	9.4	8.7	0.6	-68	-45

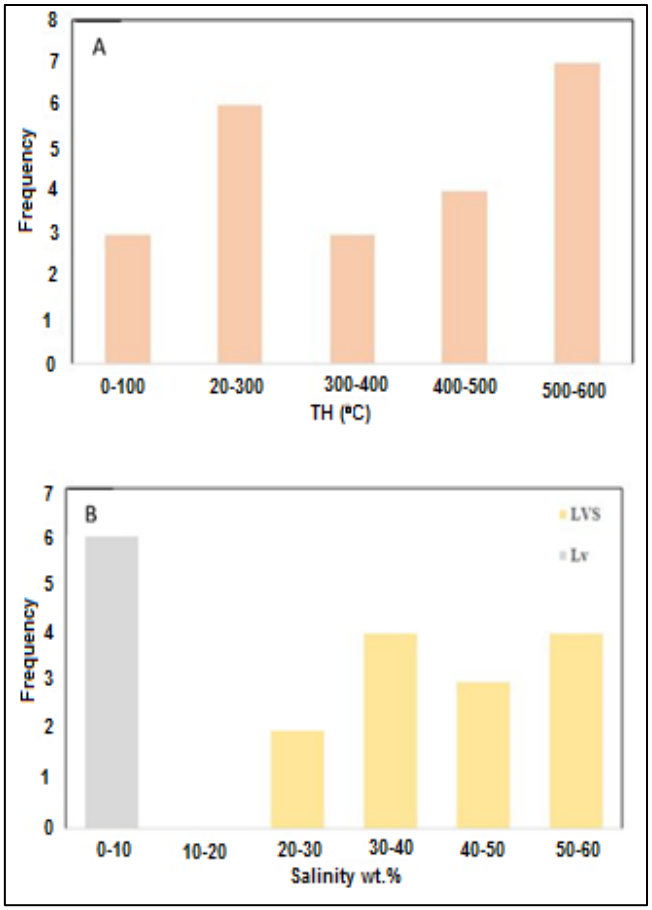

Fig. 7. Histograms of homogenization temperatures A: and salinities, and B: for fluid inclusions in different quartz veinlets from the Masjeddaghi porphyry system

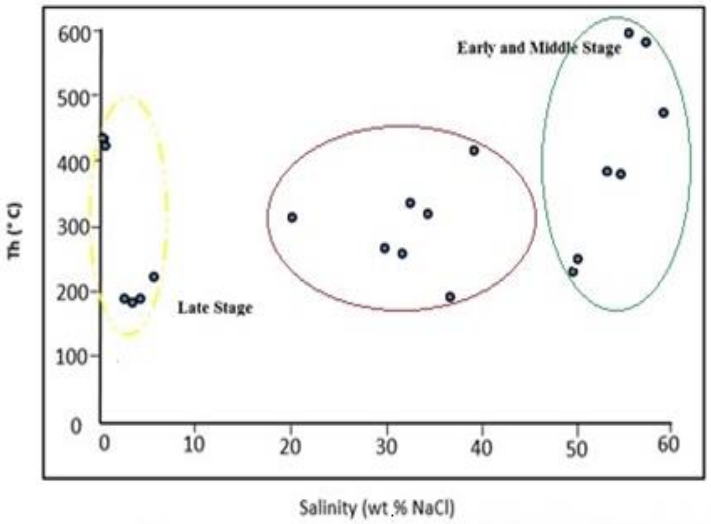

Fig. 8. Homogenization temperature vs. salinities histogram for primary fluid inclusions from the Masjeddaghi porphyry system

Table 2. The results of sulfur studies in Masjeddaghi porphyry system

Lab. Code	Sample	Mineral	Approx%S	d34S(CDT)	^{34}S
Sh-540	Msj-01-175.30	Py	42	3.7	3.1
Sh-1004	Mad-01-356.85	Cpy	45	0	-0.1
Sh-1007	Mad-03-148.30	Py	72	2.2	1.6
Sh-1008	Mad-02-405.20	Py	16	1.6	1
Sh-1010	Mad-01-159.50	Cpy	32	0.2	0.1
Sh-1013	Mad-02-349.20	Py	59	1.7	1.1
Sh-1015	Mad-02-260.70	Cpy	48	1.8	1.7
Sh-1021	Mad-01-383.90	Py	11	1.9	1.3
Sh-1025	Mad-03-262.40	Cpy	46	-0.9	-1
Mad06-254	mad06-254	Py	39	-2	-2.6
Mad09-273	mad09-273	Py	64	2	1.4
Mad09-608	mad09-608	Py	65	-1.2	1.8

Sulfur isotopes

Twelve samples (pyrite and chalcopyrite) from the depth of the Masjeddaghi porphyry system from drill holes 1, 2, 3, 6, and 9 were analyzed for sulfur isotope composition (Table 2). The value of $\delta^{34}S$ in sulfides (CDT) ranges from -2 to 3.7‰. Calculated fluid values for eight samples of pyrite in equilibrium with H_2S yielded $\delta^{34}S$ values between 3.1 and -2.6 ‰ whereas calculated fluid values for four samples of chalcopyrite in equilibrium with H_2S yielded $\delta^{34}S$ values between 1.7 and -1‰ (Ohmoto and Rye, 1979).

Four of the sulfur isotope samples are from borehole 1, three samples from borehole 2, two samples from each of boreholes 3 and 9, and one sample from borehole 6 were analyzed. Results from in boreholes 1, 2, and 3 show decreasing $\delta^{34}S$ with increasing depth in the boreholes.

The samples from borehole number 9 from the edge of the deposit near the propylitic alteration zone, have elevated $\delta^{34}S$ values, considering the location of boreholes 1, 2, and 3 in the center and borehole 9 on the edge of the ore deposit, the comparison of above data shows that the $\delta^{34}S$ values increases, considering the distance from the center of the ore deposit. Hence, the overall trend in the sulfur isotope composition shows decreases from top to the bottom and increases towards the edges.

Discussion

Fluid evolutions

Based on microthermometry analysis, quartz veinlets from deeper sections of the potassic alteration zone contain fluid inclusions with higher homogenization temperatures than those found in shallower veinlets. The range of homogenization temperatures and salinities measured from multiphase and two-phase fluid inclusions in the Masjeddaghi porphyry system is consistent with data from other giant porphyry copper systems (Wilkinson, 2001; Landtwing et al., 2010). Ebrahimi et al. (2021) further notes a strong similarity between the microthermometry data from Masjeddaghi and the Sungun mine.

Petrographic and microthermometric studies were conducted on liquid-vapor (LV) and liquid-vapor-solid (LVS) fluid inclusions from quartz and sulfide veinlets in potassic and phyllic alteration zones. The data indicate homogenization temperatures of 189–585°C and salinities of 0.3–59 wt.% NaCl equivalent. Petrographic analysis confirmed a lack of post-entrapment modification (e.g., necking down or stretching) in the halite-bearing inclusions. The spatial coexistence of high-salinity inclusions with liquid-rich and vapor-rich inclusions within the same assemblages is interpreted as primary evidence for fluid immiscibility and boiling during entrapment. (Hedenquist and Richards, 1998; Beane and Bodnar, 1995).

Based on homogenization temperature–salinity relationships, three distinct groups of fluids are identified within the Masjeddaghi system: (i) moderate to high temperature, high salinity fluids, (ii moderate temperature, moderate to high salinity fluids, and (iii) low to high temperature, low salinity fluids (Fig. 8). In this area multiphase saline fluid inclusions are similar to those in many giant porphyry systems (e.g., Roedder 1984; Cloke and Kesler, 1979), and emphasizes the presence of the high salinities and high temperatures are consistent with a magmatic resource. These fluids likely underwent boiling and were subsequently redistributed along late-stage microfracture networks. This evolution may have been influenced by variable contributions from magmatic fluids and circulating meteoric waters during progressive uplift and depressurization. (Canet et al., 2011; Dubessy et al., 2003).

In a discriminate diagram from Pirajno (2009) which has been used to explore effective ligands for metal transportation in the Masjeddaghi porphyry system. According to Fig. 9, the average measurements of the most fluid inclusions plot in the field of dominant chlorine complexes, and accordingly it could be concluded that Cl^-, HS^- and SO_4^{2-} complexes transported copper, gold and probably other elements in this porphyry system.

The mineralization process, as detailed by Wilkinson (2001), migrated from a porphyry to an epithermal setting, reflected in fluid inclusion data. Analysis reveals an inverse relationship between homogenization temperature and fluid density, and a direct relationship between salinity and density. Fluid inclusions from the potassic alteration zone display higher salinities and calculated densities (>1.0 g/cm³) compared to inclusions from the phyllic zone, which show lower density values (0.74–0.9 g/cm³).

Because of this phase separation, the homogenization temperatures are considered final trapping temperatures without need for pressure correction (Wilkinson, 2001; Roedder and Bodnar, 1980).

The pressure and depth of mineralization can be constrained through microthermometric analysis of fluid inclusions, with methodologies differing for inclusions trapped during boiling versus non-boiling conditions. Inclusions formed without boiling provide a minimum pressure constraint (Rusk et al., 2008), whereas those from boiling assemblages yield more accurate trapping pressures, as their homogenization directly reflects the pressure at the time of entrapment (Roedder and Bodnar, 1980).

Integration of microthermometric data with experimental NaCl–H_2O phase equilibrium allows estimation of trapping pressures for different stages of mineralization. This corresponds to a depth of ~1.5 km in a hydrostatic system. Subsequent stages show progressive shallowing: the middle stage (avg. Th = 266°C, 30 wt. % NaCl eq.) equilibrated at ~1 km depth, and the late stage (avg. Th = 280°C, 2.3 wt. % NaCl eq.) at <1 km.

Interpreting these pressures in terms of depth requires selecting a geological model. Assuming a lithostatic pressure regime results in depths of 1 km, 0.5 km, and <0.4 km for the early stage, middle stage, and late stage, respectively. Conversely, a hydrostatic model places these events at 1.5 km, 1.2 km, and <1.0 km (Fig. 10).

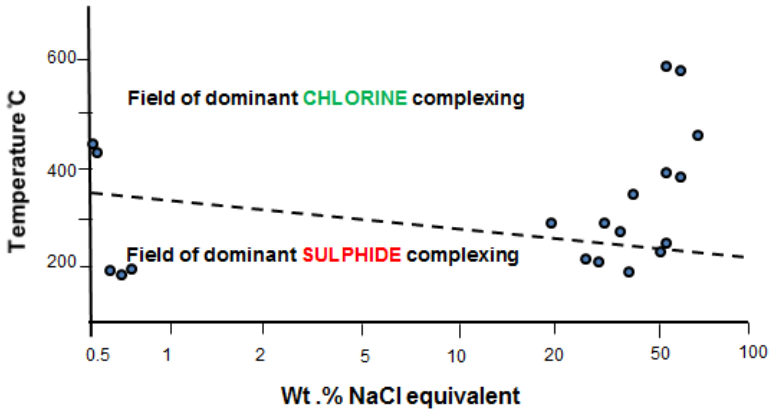

Fig. 9. Temperature vs. salinity diagrams to determin the effect of complexes (anion) transporting elements (Pirajno, 2009). According to the diagram, HS^-, SO_4^{2-}, Cl^- and HCl^- complexes were important factors of metal transportation in the Masjeddaghi porphyry system.

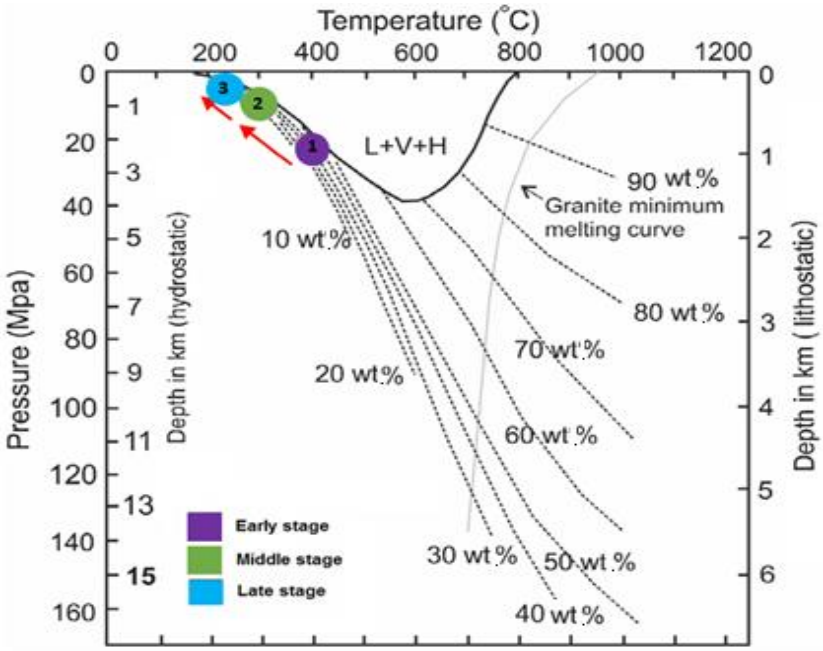

Fig. 10. Pressure and temperature diagram which shows phase relationships in the NaCl–H_2O system at hydrostatic and lithostatic pressure (Fournier, 1999). V, vapor; L, liquid; H, halite in the Masjeddaghi porphyry system. Dashed lines are contours of constant NaCl wt.% that dissolved in brines. Location of fluid inclusion assemblage in several stages have been plotted in this diagram.

Based on the research of Ebrahimi et al. (2021), two phase fluid inclusions with low salinities showed homogenization temperatures (T_h (L-V)) between 190°C and 470°C, with corresponding minimum pressures ranging from approximately 120 to 440 bars. They also identified halite-bearing (VLS-type) inclusions with higher T_h (L-V) values of 300°C to 600°C, which yielded pressures between 110 and 700 bars. These pressure data were interpreted to represent estimated depths of 0.5 to 3 km under lithostatic conditions.

Consequently, for considering the position of the potassic zone in the deep central part of a porphyry system, lithostatic pressure in the potassic zone far exceeded that in the phyllic alteration zone (the patchy alterations into andesitic country rock). Therefore, a wide range of pressure indicated by the multiphase and two phase fluid inclusions can be ascribed to a high rate of uplift and erosion in the main section in the system leading to exposure of the potassic alteration zone at surface, and trapping of two phase fluid inclusions of at lower temperature and salinity at shallower depth.

The abundance of crosscutting quartz microveinlets further indicates repeated episodes of hydraulic fracturing, consistent with episodic fluid overpressure release during porphyry evolution. The estimated mineralization depth for this deposit is approximately >0.5 to 3 km, which aligns with the typical range of 1 to 5 km for global porphyry systems (Ebrahimi et al., 2021; Pirajno, 2009). This is consistent with the general model that copper porphyry systems form at depths of 1.5 to 4 km (Sillitoe, 1973).

Fluid origin and evolution (Oxygen and hydrogen isotope data)

Different processes may affect isotopic composition of minerals in magmatic–hydrothermal fluid systems such as exsolution (Taylor, 1992), phase separation (Shmulovich et al., 1999), partial differentiation in all systems, fluid mixing or changes in temperatures or salinities (Horita et al., 1995). The intensity of hydrogen isotope fractionation to the magma differentiation ratio and the δD values of hydroxyl minerals, reflects the main fluid composition (Deering et al., 2012). Therefore, δD values of hydroxyl minerals such as biotite can be used as an indicator to determine the origin of the fluid. The δD values of hydrothermal biotites from porphyry copper deposits and magmatic waters from granodiorites vary from –30 to –60 ‰, and –40 to –80 ‰, respectively (Taylor, 1974). Factors that control the δD values of minerals are chemical compositions, temperatures of formation and/or the δD value of the fluids (Taylor, 1979).

Biotite of magmatic origin typically exhibits δD values between –60 and –100 ‰ (Kyser and O'Neil, 1982). At the Masjeddaghi porphyry system, biotites from the potassic alteration zone display δD values of –89 to –82 ‰ and $\delta^{18}O$ values of 2.3 to 3.7 ‰, which aligns with this magmatic range. The depleted δD signatures are interpreted as evidence that the hydroxyl minerals formed from a magmatic vapor that had undergone extensive degassing (Taylor, 1986). Isotopic studies indicate that in a crystallizing magma, the residual fluids become progressively depleted in deuterium. Then the process can play a key role in degassing and the subsequent formation of hydroxyl-bearing minerals during the system's final stages (Harris et al., 2015; Taylor et al., 1983). Consequently, magma degassing provides a viable explanation for both the observed δD depletions and other geochemical variations in the potassic alteration zone in a porphyry system (Harris et al., 2015).

Magma degassing in the potassic zone can deplete residual fluids in δD (Hedenquist and Richards, 1998; Richards et al., 1998). The depleted values of δD measured in biotites of the potassic zone therefore indicate that extensive volatile loss from the magma system coincided with biotite crystallization (Harris et al., 2015; Ebrahimi et al., 2021).

δD depletion in minerals from the potassic alteration zone have been reported Yukon deposit in Canada, which is interpreted as a mixture of ancient meteoric source and saline, high temperature fluids (Sheppard and Taylor, 1974; Selby and Creaser, 2001; Harris et al., 2015). The depletion trend observed in the Masjeddaghi system can be explained by the injection of high-temperature and saline magmatic waters within the hydrothermal porphyry system, a process supported by Shmulovich et al. (1999). Furthermore, the δD values of biotites in the deposit, which range from –82 to –89 ‰, are consistent with a magmatic water origin. These values can be modeled using the equation from Suzuoki and Epstein (1976), which describes the hydrogen isotope fractionation between biotite and water during mineral formation (Figs. 11 and 12).

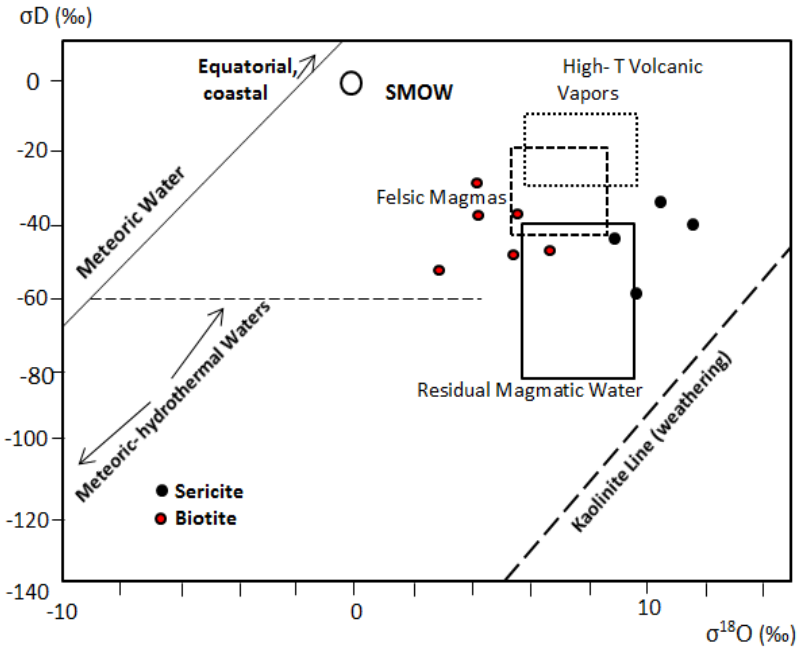

Fig. 11. Plots of $\delta^{18}O$ vs. δD data for sericite, quartz and biotite in the Masjeddaghi porphyry system. (Modified after Sheppard et al., 1971), meteoric water line after Craig (1961) and kaolinite line after Savin and Epstein (1970)

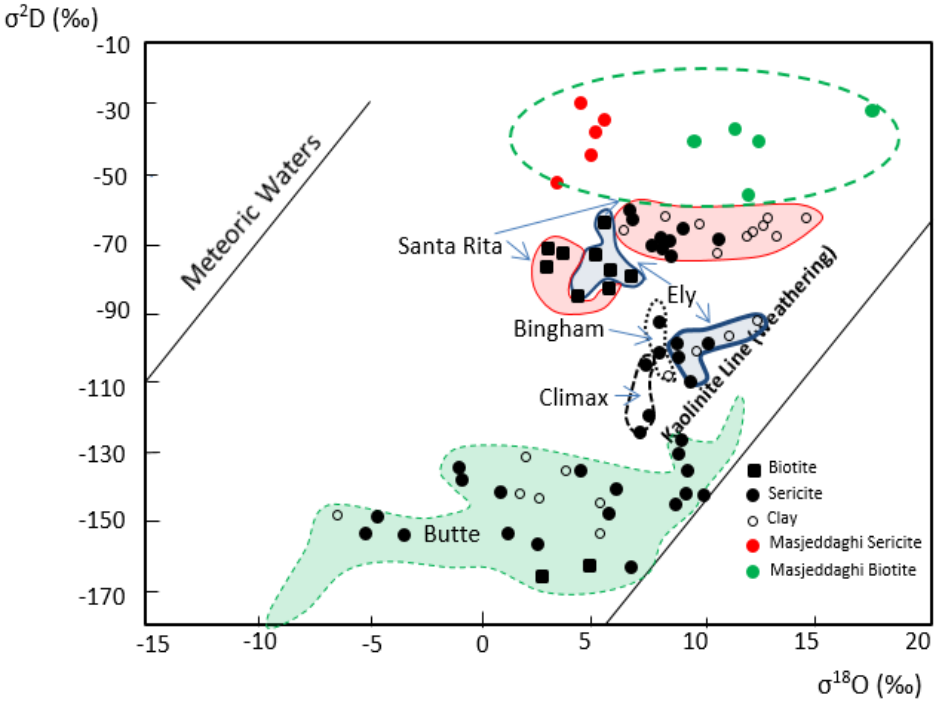

Fig. 12. Plot of δD versus $\delta^{18}O$ for sericite and biotite in the Masjeddaghi porphyry system and some giant porphyry systems. Modified after Sheppard et al. (1971) Oxygen and hydrogen and isotope ratios from above systems. Economic Geology 66: 515-542. Data for Butte are from Sheppard and Taylor (1974). Data for hypogene clays in porphyry systems are from Sheppard et al. (1969) and Savin and Epstein (1970). The meteoric water line (Craig, 1961) and kaolinite line (Savin and Epstein, 1970) shown for references. All are in Pat Shanks (2014).

Like other porphyry copper deposits, copper deposition at the Masjeddaghi porphyry system occurred in a variety of temperatures from the early potassic zone with temperatures over 580°C in diorite porphyry to surficial (patchy phyllic) alteration with temperatures ranging from 200 to 300°C in andesitic country rocks (Ebrahimi et al., 2021). Hydrogen isotope compositions of biotite from potassic alteration are interpreted to record the high-temperature magmatic-derived fluid population identified in fluid inclusions, whereas hydrogen isotopes of sericite from phyllic alteration reflect later, cooler fluids that experienced greater dilution and/or mixing.

In this research it is clear that high temperature,saline fluids had a major role in mineralization in central potassic alteration zone. Therefore, the high-temperature, high-salinity inclusion populations interpreted as boiling/immiscibility in the potassic zone are consistent with a dominantly magmatic-derived fluid reservoir inferred from biotite δD and $\delta^{18}O$ signatures.

Existence of sulfide minerals in alteration zones from many porphyry systems indicate a dominant source of metals from magma rather than country wall-rock sources. However, the analysis of stable isotopes demonstrates that the mixing and dilution of the magmatic fluid system with meteoric fluids was a terminal event in the hydrothermal system's evolution. This mixing occurred subsequent to the main copper mineralization event and only after temperatures had fallen below 200°C (Harris et al., 2015).

Fluid inclusions in quartz, as well as sulfur isotope results from the Masjeddaghi, indicate the existence of magmatic fluid sources with dilutions by meteoric water (because of its genesis), which has resulted in moderate to high salinities (40 NaCl equiv. wt.%), and sulfur isotope composition near zero per mil (-2.6 to + 3 ‰). The recorded ranges of temperature, salinity, and sulfur isotope values at Masjeddaghi are consistent with those documented in global porphyry systems. The mineral assemblage, which is rich in sulfide minerals like chalcopyrite, pyrite, and enargite, further confirms a porphyry-type deposit. The main stage of copper mineralization is characterized by an abundance of chalcopyrite and pyrite, along with secondary copper-bearing minerals. In such systems, ore-forming fluids are typically a mixture of magmatic and meteoric waters, created when magmatic vapors or brines mix with shallow groundwater. Paragenetic analysis of the Masjeddaghi system indicates that magmatic fluids were the dominant component throughout its formation (Fig. 13).

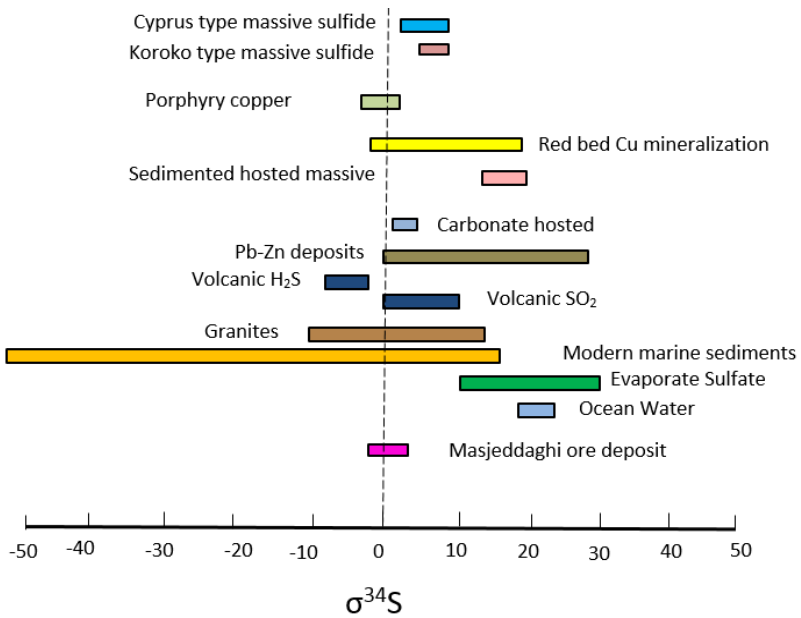

Fig. 13. $\delta^{34}S$ values of sulfide minerals from the Masjeddaghi porphyry system compared with typical ranges from other hydrothermal deposit types, illustrating the near-zero sulfur isotope signature characteristic of magmatic sulfur.

Conclusions

The Masjeddaghi porphyry system is hosted by an early Eocene diorite–diorite porphyry complex and is characterized by dominant potassic and propylitic alteration, with minor, patchy phyllic–silicic alteration. The Masjeddaghi porphyry system contains copper mineralization primarily within dominantly potassic and patches of phyllic alterations. Mineralization formed in K-feldspar, quartz stockworks, quartz veinlets, and disseminations, found in the dioritic porphyry stock and the surrounding andesitic country rocks.

The LVS fluid inclusions with high temperatures (average of Tm NaCl 400 °C) and high salinities (up to of 54 wt.% NaCl equivalent) exist in the potassic alteration zone, that indicate these alterations and association of Cu-Mo mineralization formed by a saline and high temperature fluid with a mostly magmatic origin. Homogenization temperature, salinities, pressures and densities although variable in the potassic alteration are higher than in the silicic-phyllic alteration zone.

Calculated $\delta^{18}O_{H2O}$ and δD_{H2O} values for alteration minerals are most consistent with a dominantly magmatic-derived hydrothermal system. In the Masjeddaghi porphyry, the combined fluid inclusion and isotope datasets suggest that ore-forming fluids were dominantly magmatic-derived, with increasing evidence for dilution and/or mixing with meteoric water during later phyllic-silicic stage evolution. This is evidenced by the silicic-phyllic alteration zone, which formed at temperatures between 300° and 400°C and exhibits stable isotope signatures of low δD values (–60 ‰) and moderate to high $\delta^{18}O$ values (8.7 to 11.9 ‰). The $\delta^{34}S$ values can be another event which increases, from the center of the porphyry system to the edge and decreases from top to the bottom, and are in consistent with typical porphyry copper systems. Together, all these results support a porphyry-style genetic model in which high-temperature saline magmatic fluids were the primary agents of Cu–Au mineralization, followed by late-stage fluid evolution during uplift and erosion.

Conflict of Interest

The authors declare that they have no conflict of interest.

Acknowledgment

This research was funded by "Exploration Department" at NICICO (National Iranian Copper Industries Company). Supports by Mohammad Kargar and Mehrdad Heidari, ex-administrators of "Exploration and Engineering Development Department", were a prerequisite for initiation and completion of the research. We thank Kerry Klassen at the Queens University, and the staff for their assistance in Stable Isotope Lab Manager QFIR, Geological Sciences, 36 Union St.Kingston, Ontario, Canada, in analytical procedures. The authors' gratitude is further expressed to Dr. Peter Pollard (Australia), for reviewing of the manuscript and making critical comments and valuable suggestions and the authors appreciate the very helpful suggestions and comments by the chief editor professor Mohammad Hassan Karimpour, Dr. Azadeh Malekzadeh and very thanks to Sara Habibi from the Journal of Economic Geology.

References

Akbarpour, A., 2005. Economic Geology of Kiamaki Area Regarding Gold and Copper Mineralization (Masjeddaghi Jolfa) in Eastern Azerbaijan. Ph.D. Thesis, Science and Research Branch, Islamic Azad University, Tehran, 262 pp.

Atalou, S, Nazafati, N., Lotfi, M. and Aghazadeh, M., 2017. Fluid inclusion investigations of the Masjeddaghi copper-gold porphyry-epithermal mineralization, east Azerbaijan province, NW Iran. Open Journal of Geology, 7(8):1 110–1127. https://doi.org/10.4236/ojg.2017.78074

Beane, R.E. and Bodnar, R.J., 1995. Hydrothermal fluids and hydrothermal alteration in porphyry copper deposits. In: F.W. Pierce and J.G. Bohm (Editors), Porphyry copper deposits of the American Cordillera: Arizona. Geological Society Retrieved February 20, 2026 from https://www.scirp.org/reference/referencespapers?referenceid=1779985

Bottinga, Y. and Javoy, M., 1975. Oxygen isotope partitioning among the minerals in igneous and metamorphic rocks. Rev. Journal of Geophysical research: Space Physics, 13: 401–418. https://doi.org/10.1029/RG013i002p00401

Brenan, J.M., Shaw, H.F., Phinney, D.L. and Ryerson, F.J., 1994. Rutile aqueous fluid partitioning of Nb, Ta, Hf, Zr, U and Th: Implications for high field strength element depletions in island arc basalts. Earth and Planetary Science Letters, 128(3–4): 327–339. https://doi.org/10.1016/0012-821X(94)90154-6

Calagari, A.A., 2004. Fluid inclusion studies in quartz veinlets in the porphyry copper deposit at Sungun, East–Azarbaidjan, Iran. Journal of Asian Earth Sciences, 23(2): 179–189. https://doi.org/10.1016/S1367-9120(03)00085-3

Canet, C., Franco, S.I., Prol–Ledesma, R.M., González–Partida, E. and Villanueva–Estrada, R.E., 2011. A model of boiling for fluid inclusion studies: application to the Bolaños Ag–Au–Pb–Zn epithermal deposit, Western Mexico. Journal of Geochemical Exploration, 110(2–11): 118–125. https://doi.org/10.1016/j.gexplo.2011.04.005

Cloke, P.L. and Kesler, S.E., 1979. The halite trend in hydrothermal solutions. Economic Geology, 74(8): 1823–1831. https://doi.org/10.2113/gsecongeo.74.8.1823

Craig, H., 1961. Isotopic variations in meteoric waters. Science, 133(3465): 1702–1703. https://doi.org/10.1126/science.133.3465.1702

Davidson, J.P., 1996. Deciphering mantle and crustal signatures in subduction zone magmatism. Geophysical Monograph, 96(2): 251–262. https://doi.org/10.1029/GM096p0251

De Hoog, J.C.M., Mason, P.R.D. and van Bergen, M. J., 2001. Sulfur and chalcophile elements in subduction zones: Constraints from a laser ablation ICP-MS study of melt inclusions from Galunggung Volcano, Indonesia. Geochimica et Cosmochimica Acta, 65(18): 3147–3164. https://doi.org/10.1016/S0016-7037(01)00634-2

Deering, C.D., Horton, T.W., Gravley, D.M. and Cole, J.W., 2012. Hornblende, cummingtonite, and biotite hydrogen isotopes: Direct evidence of slab–derived fluid flux in silicic magmas of the Taupo Volcanic Zone, New Zealand. Journal of Volcanology and Geothermal Research, 233-234: 27–36. https://doi.org/10.1016/j.jvolgeores.2012.04.010

Dilles, J., 1992. Wall-rock alteration and hydrothermal flow paths about the Ann-Mason porphyry copper deposit, Nevada; a 6-km vertical reconstruction. Economic Geology, 87(8): 1963–2001. https://doi.org/10.2113/GSECONGEO.87.8.1963

Dubessy, J., Derome, D. and Sausse, J., 2003. Numerical modeling of fluid mixings in the H2O–NaCl system application to the North Caramal U prospect (Australia). Chemical Geology 194(1–3): 25–39. https://doi.org/10.1016/S0009-2541(02)00269-3

Ebrahimi, S., Pan, Y. and Rezaeian, M., 2021. Origin and evolution of the Masjeddaghi Cu-Au-Mo porphyry and gold epithermal vein system, NW Iran: Constraints from fluid inclusions and sulfur isotope studies. Mineralogy and Petrology, 115(6): 643–66. https://doi.org/10.1007/s00710-021-00761-z

Foley, S.F., Barth, M.G. and Jenner, G.A., 2000. Rutile/melt partition coefficients for trace elements and an assessment of the influence of rutile on the trace element characteristics of subduction zone magmas. Geochimica et Cosmochimica Acta, 64(5): 933–938. https://doi.org/10.1016/S0016-7037(99)00355-5

Fournier, R.O., 1999. Hydrothermal processes related to movement of fluid from plastic into brittle rock in the magmatic–epithermal environment. Economic Geology, 94(8): 1193–1211. https://doi.org/10.2113/gsecongeo.94.8.1193

GSI, 1999. Geological map of the Masjeddaghi in scale 1:2000. unpublished interior report.

Gustafson, L.B. and Hunt, J.P., 1975. The_Porphyry_Copper_Deposi_at_El_Salvador _Chile. Economic Geology, 70(5): 857–912. https://doi.org/10.2113/gsecongeo.70.5.857

Harris, A.C., Golding, S.D. and White., N.C., 2015. Bajo de la Alumbrera copper-gold deposit: Stable isotope evidence for a porphyry-related hydrothermal system dominated by magmatic aqueous fluids. Economic Geology, 100(5): 863–886. https://doi.org/10.2113/100.5.863

Hassanpour, S., 2010. Metallogeny and Mineralization of Cu–Au in Arasbaran Zone (NW Iran), Ph.D. Thesis, University of Shahid Beheshti, Tehran, 323 pp.

Hassanpour, S. and Ebrahimi, S., 2023. Stable isotope (S-H-O) studies on Astamal deposit: Indication to mineralized fluid resources, NW Iran. Scientific Quarterly Journal of Geosciences, 33(3):201–218. (in persian with English Abstract) https://doi.org/10.22071/gsj.2023.375717.2041

Hassanpour, S., Alirezaei. S, Selby. D. and Sergeev, S., 2015. SHRIMP zircon U–Pb and biotite and hornblende Ar–Ar geochronology of Sungun, Haftcheshmeh, Kighal, and Niaz porphyry Cu–Mo systems: evidence for an early Miocene porphyry–style mineralization in northwest Iran.

International Journal of Earth Sciences, 104(1): 45–59. https://doi.org/10.1007/s00531-014-1071-0

Hassanpour, S., Rahnama, Z. and Ebrahimi, S., 2022. Determination of physicochemical conditions of causative intrusion in the Masjeddaghi Cu-Au porphyry-epithermal deposit: constraints on chemical composition of biotite. Journal of Economic Geology, 14(4): 149–174. (in Persian with English abstract) https://doi.org/10.22067/econg.2023.79377.1056

Hassanpour, S. and Rajabpour, S., 2019. The Kighal Porphyry Cu–Mo Deposit, NW Iran: Insights into Origin and Evolution of the Mineralizing Fluids. Russian Geology and Geophysics, 60(10): 1141–1162. https://doi.org/10.15372/RGG2019115

Hassanpour, Sh. and Alirezaei, S., 2017. Eocene Masjeddaghi porphyry Cu-Au deposit; an example of island arc porphyry type deposit in NW Iran. Scientific Quarterly Journal of Geosciences, 26(104): 43–58. (in ersian with English abstract) https://doi.org/10.22071/gsj.2017.50166

Hedenquist, J.W. and Richards, J.P., 1998. The influence of geochemical techniques on the development of genetic models for porphyry copper deposits. In: J.P. Richards and P.B. Larson (Editors), Techniques in hydrothermal ore deposits geology, V. 10. Society of Economic Geologists. https://doi.org/10.5382/Rev.10.10

Horita, J., Cole, D.R. and Wesolowski, D.J., 1995. The activity–composition relationship of oxygen and hydrogen isotopes in aqueous salt solutions: III. Vapor–liquid water equilibration of NaCl solution to 350°C. Geochimica et Cosmochimica Acta, 59(6): 1139–1151. https://doi.org/10.1016/0016-7037(95)00031-t

IMPRC, 2026. Fluid Inclusion studies of Samples from NW of Iran. Iran Mineral Processing Research Center in Karaj, Iran. Retrieved February 20, 2026 from http://www.imprc.ir/%D8%AE%D8%AF%D9%85%D8%A7%D8%AA-%D8%A2%D8%B2%D9%85%D8%A7%DB%8C%D8%B4%DA%AF%D8%A7%D9%87%DB%8C-%D9%85%D8%B1%DA%A9%D8%B2/%DA%A9%D8%A7%D9%86%DB%8C-%D8%B4%D9%86%D8%A7%D8%B3%DB%8C

Kusakabe, M., Shingo, M. and Nakamura, E., 1990. S, O and Sr isotope systematics of active vent materials from the Mariana back arc basin spreading axis at 18°N. Earth and Planetary Science Letters, 100(1–3): 275-282. https://doi.org/10.1016/0012-821X(90)90190-9

Kyser, T.–K. and O'Neil, J.R., 1982. Genetic relations among basic lavas and ultramafic nodules: evidence from oxygen isotope compositions. Contribution to Mineralogy and Petrology, 81: 88–102. https://doi.org/10.1007/bf00372046

Landtwing, M.R., Furrer,C., Redmond, P.B., Pettke, T., Guillong M. and Heinrich, C.A., 2010. The Bingham Canyon porphyry Cu–Mo–Au deposit: III. Zoned coper–gold ore deposition by magmatic vapor expansion. Economic Geology, 105(1): 91–118. https://doi.org/10.2113/gsecongeo.105.1.91

NICICO. 2008. Final exploration Report on Masjeddaghi area. National Iranian copper industries company, not published. (in Persian)

Ohmoto, H. and Rye, R.O., 1979. Isotope of sulfur and carbon. In: H.L. Barnes (Editor), Geochemistry of Hydrothermal deposits, John Wiley & Sons, pp. 509–567. Retrieved February 20, 2026 from https://cir.nii.ac.jp/crid/1573105975177859072

Pat Shanks, W.C., 214. Stable Isotope Geochemistry of Mineral Deposits. Treatise on Geochemistry (Second Edition), 13: 59–82. https://doi.org/10.1016/B978-0-08-095975-7.01103-7

Pirajno, F., 2009. Hydrothermal processes and mineral systems. Geological Survey of Western Australia, Springer, 1250 pp. Retrieved February 20, 2026 from http://link.springer.com/book/10.1007/978-1-4020-8613-7

Richards, J.P., Krogh, T.E. and Spooner, E.T.C., 1998. Fluid inclusion characteristics and U–Pb rutile age of late hydrothermal alteration and veining at the Musoshi stratiform copper deposit, Central African copper belt, Zaire. Economic Geology 83(1): 118–139. https://doi.org/10.2113/gsecongeo.83.1.118

Roedder, E., 1984. Fluid inclusions. Mineral Society of America, V. 12. Mineralogical Society of America, PP. 644.

Roedder, E. and Bodnar, R.J., 1980. Geologic pressure determination from fluid inclusion studies. Annual Review of Earth and Planetary

Science 8: 263–301. https://doi.org/10.1146/annurev.ea.08.050180.001403

Rusk, B.G., Reed, M.H. and Dilles, J.H., 2008. Fluid inclusion evidence for magmatic–hydrothermal fluid evolution in the porphyry copper–molybdenum deposit at Butte, Montana. Economic Geology 103(2): 307−334. https://doi.org/10.2113/gsecongeo.103.2.307

Savin, S.M. and Epstein, S., 1970. The oxygen and hydrogen isotope geochemistry of clay minerals. Geochimica et Cosmochimica Acta, 34(1): 25–42. https://doi.org/10.1016/0016-7037(70)90149-3

Selby, D. and Creaser, R.A., 2001. Re–Os Geochronology and Systematics in Molybdenite from the Endako Porphyry Molybdenum Deposit, British Columbia, Canada. Economic Geology 96:197–204. https://doi.org/10.2113/96.1.197

Sheppard, S. M. F., Gustafson, L. B., 1976. Oxygen and hydrogen isotopes in the porphyry copper deposit at El Salvador, Chile. Economic Geology, 71(8): 1549–1559. https://doi.org/10.2113/gsecongeo.71.8.1549

Sheppard, S.M.F., Nielsen, R.L and Taylor, H.P. Jr., 1969. Oxygen and hydrogen isotope ratios of clay minerals from porphyry copper deposits. Economic Geology, 64(7): 755–777. https://doi.org/10.2113/gsecongeo.64.7.755

Sheppard, S.M.F., Nielsen, R.L. and Taylor, H.P.Jr., 1971. Hydrogen and oxygen isotope ratios in minerals from porphyry copper deposits. Economic Geology, 66(4): 515−542. https://doi.org/10.2113/gsecongeo.66.4.515

Sheppard, S.M.F. and Taylor, H.P., JR., 1974. Hydrogen and oxygen isotope evidence for the origin of water in the Boulder batholoth and the Butte ore deposit, Montana. Economic Geology, 69(6): 926–946. https://doi.org/10.2113/gsecongeo.69.6.926

Shepherd, T., Rankin, A.H. and Alderton, D.H.M., 1985. A Practical Guide to Fluid Inclusion Studies. Blackie, London, 239 pp. Retrieved February 20, 2026 from http://books.google.com/books/about/A_Practical_Guide_to_Fluid_Inclusion_Stu.html?id=CVSGAAAAIAAJ

Shmulovich, K.I., Landwehr, D., Simon, K. and Heinrich, W., 1999. Stable isotope fractionation between liquid and vapor in water–salt systems up to 600°C. Chemical Geology, 157(3): 343–354. Retrieved February 17, 2026 from https://repository.geologyscience.ru/handle/123456789/23066

Sillitoe, R.H., 1973. The tops and bottoms of porphyry copper deposits. Economic Geology, 68(6): 799–815. https://doi.org/10.2113/gsecongeo.68.6.799

Stocklin, J. and Setudehnia, A., 1972. Lexique Stratigraphique International Volume III, ASIE centnational de la Recherche scientifique. 15 quai Anodle-France 75 (paris-VII), Geological Survey of Iran, Report no. 18, second edition, 376 pp. Retrieved February 20, 2026 from https://www.sudoc.abes.fr/cbs/DB=2.1//SRCH?IKT=12&TRM=002208075

Suzuoki, T. and Epstein, S., 1976. Hydrogen isotope fractionation between H-bearing minerals and water. Geochimica et Cosmochimica. Acta, 40(10): 1229–1240. https://doi.org/10.1016/0016-7037(76)90158-7

Taylor, B.E.. 1986. Chapter 7. Magmatic volatiles: Isotopic variation of C, H, and S. In: J.W. Valley, H.P. Taylor and J.R. O'Neil (Editors), Stable Isotopes in High Temperature Geological Processes, Berlin, Boston: De Gruyter, pp. 185-226. https://doi.org/10.1515/9781501508936-012

Taylor, B.E., 1992. Degassing of H2O from rhyolite magma during eruption and shallow intrusion, and the isotopic composition of magmatic water in hydrothermal systems. In: J.W. Hedenquist (Editor), Magmatic contributions to hydrothermal systems, Geological Survey of Japan Report 279, pp. 190–195. Retrieved February 20, 2026 from http://darc.gsj.jp/archives/detail?cls=geolis&pkey=199207792

Taylor, B.E., Eichelberger, J.C. and Westrich, H.R., 1983. Hydrogen isotopic evidence of rhyolitic magma degassing during shallow intrusion and eruption. Nature, 306: 541–545. https://doi.org/10.1038/306541a

Taylor, H.P., 1974. The application of oxygen and hydrogen isotope studies to problems of hydrothermal alteration and ore deposition. Economic Geology; 69(6): 843−883. https://doi.org/10.2113/gsecongeo.69.6.843

Taylor, H.P., 1979. Oxygen and hydrogen isotope relationships in hydrothermal mineral deposits. In: H.L. Barnes (Editor), Geochemistry of hydrothermal ore deposits, Wiley, New York, pp.

236–277, Retrieved February 20, 2026 from https://books.google.com/books/about/Geochemistry_of_Hydrothermal_Ore_Deposit.html?id=vy2_QnyojPYC

Whitney, D.L. and Evans, B.D.W., 2010. Abbreviations for names of rock-forming minerals. American Mineralogist, 95(1): 185–187. https://doi.org/10.2138/am.2010.3371

Wilkinson, J.J., 2001. Fluid inclusions in hydrothermal ore deposits. Lithos, 55(1–4): 229–272. https://doi.org/10.1016/S0024-4937(00)00047-5

Zhang, Y.G. and Frantz, J.D., 1987. Determination of the homogenization temperatures and densities of supercritical fluids in the system NaCl–KCl–$CaCl_2$–H_2O using synthetic fluid inclusions. Chemical Geology 64(3–4): 335–350. https://doi.org/10.1016/0009-2541(87)90012-X

Zheng, Y.F., 1993. Calculation of oxygen isotope fractionation in hydroxyl–bearing silicates. Earth and Planetary Science Letter, 120(3–4): 247–263. https://doi.org/10.1016/0012-821X(93)90243-3

دوره ۱۸، شماره ۱، ۱۴۰۵، صفحه ۱۴۹ تا ۱۶۹ شاپا چاپی: ۷۳۰۶-۲۰۰۸ شاپا الکترونیکی: ۵۸۶۵-۲۴۲۳

زمین‌شناسی اقتصادی

https://econg.um.ac.ir

مقاله پژوهشی 10.22067/econg.2026.1164 OPEN ACCESS

بررسی تکامل سیالات گرمابی بر اساس مطالعه ایزوتوپ‌های پایدار (اکسیژن، هیدروژن، گوگرد) و سیالات درگیر در کانسار پورفیری (مس- طلا) مسجدداغی، شمال‌غرب ایران

شهره حسن‌پور [۱*]، سید جواد مقدسی [۲]

[۱] دانشیار، گروه زمین‌شناسی، دانشگاه پیام نور، تهران، ایران

[۲] دانشیار، گروه زمین‌شناسی، دانشگاه پیام نور، تهران، ایران

اطلاعات مقاله

تاریخ دریافت: ۱۴۰۴/۰۹/۱۰

تاریخ بازنگری: ۱۴۰۵/۰۲/۰۲

تاریخ پذیرش: ۱۴۰۵/۰۲/۰۷

واژه‌های کلیدی

سولفور

ایزوتوپ‌های اکسیژن و هیدروژن

میکروترمومتری سیالات درگیر

مسجدداغی

شمال‌غرب ایران

نویسنده مسئول

شهره حسن‌پور

hassanpour@pnu.ac.ir

چکیده

کانسار مسجدداغی، واقع در شمال‌غربی ایران، شامل یک سامانه مس- طلای پورفیری است که از نظر مکانی با جایگزینی رگه‌های سیلیسی اپی‌ترمال و کانی‌سازی طلا در ارتباط است. کمپلکس نفوذی- آتشفشانی در این منطقه در اوایل ائوسن با ترکیب متغیر از کوارتز- دیوریت تا دیوریت تشکیل‌شده است. از نظر زمین‌شیمیایی، گرانیتوئید منطقه مربوط به محیط‌های جزایر کمانی است و به دلیل آلودگی گوشته‌ای در ارتباط با فرورانش، از عناصر لیتوفیل یون بزرگ مانند Y، Th، Rb، Ba و Cs غنی‌شده است. سیالات درگیر اولیه در رگچه‌های پورفیری در دماهای مختلف از ۱۸۹ تا ۵۸۵ درجه سانتی‌گراد به صورت مایع و بخار همگن شده‌اند و شوری بین بیش از ۰/۳ تا ۵۹ درصد وزنی معادل NaCl را نشان می‌دهند که نشان‌دهنده جوشش سیال و تفکیک فازهاست. سیالات با ایزوتوپ هیدروژن سنگین ۶۰ - تا-۳۰ ‰ و ایزوتوپ‌های سنگین اکسیژن $\delta^{18}O$ ۴/۳ تا ۱۱/۹‰، نشان‌دهنده منشأ ماگمایی غالب سیالات در مقایسه با دخالت محدود آب‌های جوی است. این نتایج نشان می‌دهد که سیالات ماگمایی شور و با دمای بالا نقش اصلی را در کانی‌سازی مس- طلا در مسجدداغی ایفا کرده‌اند.

استناد به این مقاله

حسن‌پور، شهره و مقدسی، سیدجواد، ۱۴۰۵. بررسی تکامل سیالات گرمابی بر اساس مطالعه ایزوتوپ‌های پایدار (اکسیژن، هیدروژن، گوگرد) و سیالات درگیر در کانسار پورفیری (مس- طلا) مسجدداغی، شمال‌غرب ایران. زمین‌شناسی اقتصادی، ۱۸(۱): ۱۴۹-۱۶۹. https://doi.org/10.22067/econg.2026.1164